M.S. DISSERTATION

Growth of GaN thin film on the sapphire covered by hexagonal non-closed packed hollow silica particles

Jin Lu

August 2014

DEPARTMENT OF MATERIALS SCIENCE AND ENGINEERING

COLLEGE OF ENGINEERING

SEOUL NATIONAL UNIVERSITY

Growth of GaN thin film on the sapphire covered by hexagonal non-closed packed hollow silica particles

지도 교수 윤 의 준

이 논문을 공학석사 학위논문으로 제출함

2014 년 8 월

서울대학교 공과대학원

재료공학부

김로

김로의 석사학위논문을 인준함

2014년 8 월

위 원 장 주 영 창 (인)

부위원장 윤 의 준 (인)

위 원 박 용 조 (인)

Abstract

In few decades, III-V compound semiconductors have attracted much attention due to theirs excellent optical properties. Especially, because of the suitable band gap of GaN, it is selected and used in the light emitting diode (LED) devices. Comparing with conventional lighting devices, LED devices have many advantages, such as high lighting efficiency, long lifetime of devices, and less heating lighting effect. However, the performance of conventional GaN based LED devices is suffered by high threading dislocation density, low external extraction efficiency and wafer bowing effect.

In order to overcome these problems, a method of growth of GaN thin film on the sapphire covered by hexagonal non-closed packed (HNCP) hollow silica particles was proposed in this study. This method concluded three steps. At first, various sized monodisperse shrinkable PS-silica core-shell beads were synthesized. As-synthesized particles had two important features, one was the shrinkable shell, and another was decomposable core. Second step was patterning. Sapphire substrate coated by monolayer core-shell particles with hexagonal closed packed (HCP) structure was fabricated by spin-coating method. Then after thermal treatment, HCP core-shell particles array was transformed to HNCP hollow silica particles array. The main defects in HNCP silica hollow particle pattern was the connection between particles. Due to connection between neighboring particles, HNCP pattern was not perfect.

These connection defects were inevitably formed during thermal treatment with low ramping time. However in the case of thermal treatment with high ramping time, connection between neighboring particles could be avoided. In the end, GaN thin film was grown on patterned substrate by metal organic chemical vapor deposition (MOCVD). Due to high coverage percentage of hollow silica beads mask, existence of bilayer and aggregate particles, and imperfect growth condition, GaN films was not fully coalescent. SEM images show that self-assembly HNCP hollow silica particle pattern was successfully embedded with GaN thin films with ultra-high coverage percentage of hollow silica beads. By using HNCP hollow silica beads coated substrate, XRD FWHM value of (102) plane was reduced from 521.1 to 335.1 arcsec, PL intensity was increased by a factor of 7, the PL peak was shift from 361.8 to 363.5. We concluded that GaN films are grown with higher crystal quality, higher external quantum efficiency and lower stress by inserting HNCP hollow silica beads.

Key Words:

Metal organic chemical vapor deposition (MOCVD), Gallium nitride (GaN), Hexagonal non-closed packing (HNCP), Shrinkable polystyrene-silica core-shell beads, Hollow silica beads, Spin coating, Thermal treatment

Student Number: 2012-23925

Contents

List of Figures

Chapter 1. Introduction

In few decades, III-V compound semiconductors, such as gallium nitride (GaN), aluminum nitride (AlN), indium nitride (InN) have attracted much attention due to theirs excellent optical properties. Especially, because of the suitable band gap of GaN, it is selected and used in the light emitting diode devices (LED).[1] Comparing with other conventional lighting devices, LED devices have many advantages, such as high lighting efficiency, long lifetime of devices, and less heating lighting effect. The limited source of fossil fuel on the earth and growing consuming of energy of human being is a serious problem need to be solved urgently. Under these circumstances, there is a tendency to replace all of the incandescent lamps by high efficacy lighting devices to reduce the energy consumption. The huge market and urgent demanding around the world impels the companies and research institutions to investigate the methods of growing high-quality and low-cost GaN thin films.

In the case of growth of GaN, homoepitaxy is a very difficult and high-cost work due to the hardship of fabrication of GaN substrate.[2] Because of the high melting point and slow growth speed, the cost of using Czochralshi method is extremely high, which is the most conventional method of growth of bulk single crystal. By these reasons, the heteroepitaxy [3] of GaN on other different substrate is the main method of current research tendency. For example, metal organic chemical vapor deposition (MOCVD) is usually used to grow GaN thin films, on various substrates like sapphire, Si, and SiC substrates

as heteroepitaxial growth.[4~7]

Although using the heteroepitaxial growth to fabricate GaN thin films solve the problem of high cost in the fabrication process, the performance of the devices are still suffered by poor crystal quality of GaN epitaxial layer. There are three main problems of the heteroepitaxial layer. First problem is the high threading dislocation density in the GaN thin films. Due to the large lattice mismatch between sapphire substrate and GaN epitaxial layer, the stress is accumulated from the interface to epitaxial layer. Finally, huge amount of threading dislocations are formed when the thickness of thin films is great than critical thickness. In the case of sapphire substrate, lattice mismatch is 15% [8], the density of threading dislocation is as high as 10^{9}~^{11}cm^{-2} without any special growth method. Thus, dislocations in the GaN thin films work as non-radiative recombination centers to catch and kill carriers.[9~11] By this reason, finding a strategy to reduce density of dislocation is a very necessary and effective method to improve the efficiency of LED devices. Second problem is low external extraction efficiency of GaN based LED devices. Comparing with refractive index of air (n_{air}=1.0), refractive index of GaN is too large (n_{GaN}=2.43). Most of the photons generated in the semiconductor films are not able to escape to the air. This is so-called total internal reflection. According to the Snell's law, only when the incident angle of photon is smaller than 23.6°, photon is able to escape from semiconductor, if not photon will be trapped in the semiconductor.[12] In other word, only 4.2% of total photon is able to be extracted from escape cone. This means that, if we want to increase total

lighting efficiency of devices, we have to increase external quantum efficiency by certain design of device structure. Third problem is wafer bowing. Due to large difference of thermal expansion coefficient between sapphire substrate and GaN epitaxial layer, after growth at high temperature, bowing of wafer happens at room temperature. It will increase cost and lower quality of production.[13]

In order to solve these problems of conventional GaN based LED devices, a lot of effective methods were proposed. One of the most famous methods is named as lateral epitaxial overgrowth (LEO).[14,15] Process of LEO can be described as follow. At first, a dielectric material such as silica or silicon nitride was deposited on the substrate as a mask with certain amount of opening space on the bare substrate. Mask region, which was not able to grow GaN nuclei on it, is fabricated generally by photolithographic techniques. Because of this selective epitaxial growth mode, GaN was grown only on the opening windows. Then by adjusting growth condition, growth mode was transformed to lateral epitaxial growth, and dielectric mask was finally covered by GaN films by coalesce of GaN islands. After LEO process, GaN thin film with full coalescence state and smooth surface was grown. Due to the reducing of contact region between substrate and epitaxial layer and annihilated dislocations which were bended to lateral direction and encountered with each other, threading dislocation density was reduced greatly by LEO. However, because of complicated fabrication process, cost of this technique is quite high. Other well-known method to fabricate high efficiency LED devices is patterned

sapphire substrate (PSS).[16~19] The idea of this method was using uneven substrate to increase possibility of extraction of photon by scattering effect. PSS was generally fabricated by reactive ion etching. Similar with the case of LEO, GaN films was selectively grown on the substrate without patterns. This means that PSS can not only reduce dislocation density, but also increase external quantum efficiency. However, this method is also very complicated and expensive. Recently, using silicon or sapphire substrate coated by monolayer of silica beads as mask to grow high quality GaN thin films was reported by several group.[20~23] Existence of silica beads not only worked as mask to reduce dislocation density, but also increased external quantum efficiency by scattering effect. In order to further remove stress of GaN epitaxial film, meanwhile utilize silica beads to reduce density of dislocation and increase external quantum efficiency, one of seniors in our group, Jonghak Kim reported a method of using hollow silica monolayer coated sapphire as substrate to grow GaN thin films. Experiment result showed that stress of epitaxial films is also greatly reduced by this method.[13]

In this paper, a method of growth of GaN thin film on the sapphire covered by hexagonal non-closed packed monolayer hollow silica particles is proposed. This method concludes three steps. At first, various sized monodisperse shrinkable PS-silica core-shell beads are synthesized. Size of core-shell bead can be adjusted from 300nm to 3μm. The as-synthesized particles have two important features, one is shrinkable shell, and another is decomposable core. After thermal treatment at high temperature in the air, size of silica shell

becomes smaller, meantime, PS core is removed and spherical shape is remained. Core-shell particle is transformed into hollow silica shell with a smaller size than as-synthesized beads. Then second step is patterning. Sapphire substrate coated by monolayer core-shell particles with HCP structure is fabricated by spin-coating method. Then after thermal treatment, HCP core-shell particles array is transformed to HNCP hollow silica particles. However, due to connection between neighboring particles, HNCP pattern is not perfect. In the end, GaN thin film is grown on patterned substrate by MOCVD method.

The highlights of this research are shown as follow. At first, polystyrene-silica core-shell beads with various sizes from 3μm to 300nm are synthesized by one-pot methods instead of two-step reaction to reduce cost and process. HNCP hollow silica array is coated on the bare sapphire substrate with controllable coverage percentage from 50% to 85% to further reduce stress. Compare with other patterning method of HNCP hollow particles array, our fabrication process is greatly simple and low-cost. In the end, instead of totally random packed particles, our coated sample has some degree of periodic structure. Although not perfect, this periodic structure can increase external quantum efficiency.

Chapter 2. Synthesis of shrinkable core-shell sphere by one-pot method

2.1 Introduction

2.1.1 Synthesis of polystyrene-MTC copolymer

There are two different kinds of polymerization reaction depending on the reaction product of the polymerization procedure. First one is addition polymerization; sometimes it is called chain reaction polymerization. During the process of addition polymerization, polymer is the only production of reaction. Other is condensation polymerization or step reaction polymerization. In this case, during the polymerization, not only large molecule like polymer but also small molecule like water, is formed. Polymerization of polystyrene-2-(methacryloyl)ethyltrimethylammonium chloride (polystyrene-MTC) is an addition polymerization. During reaction process, the double bond of both styrene and MTC breaks and then monomer connects with each other to form a long chain molecule. In our experiment, double bond between carbon atoms in both styrene and MTC molecules is broken in polymerization reaction. Then a long chain molecule is formed with a random arranged structure like -A-A-B-A-A-A-B-A-…, which A and B represent styrene and MTC, respectively. In Fig.1, the molecular structure of styrene, MTC, and copolymer is shown, respectively.

In the case of addition polymerization, existence of initiator is necessary. In general, one or more chemical bond of initiator molecule breaks at the beginning of reaction and produces several small molecules with an unpaired electron, named as radical or highly active ion depending on the charge of active atom. If polymerization is initiated by small molecules with an unpaired electron, it is called as free radical polymerization. On the other hand, in the case of polymerization is initiated by highly active ion, it is called as ionic polymerization.

In our experiment, azoic compound is selected as initiator. This kind of compound is not stable in high temperature, single bond between carbon and nitrogen breaks, and decomposes into N_2 gas and two radicals. Radical is a species which has one or more unpaired valence electrons. It has a tendency to gain electron, or form a chemical bond with other atoms. Because of this reason, initiator radicals react with the monomer and produce monomeric radicals. By the chain reaction between radicals and monomer, the monomeric radicals continually propagate to form oligomeric radicals. Polystyrene-MTC copolymer molecules precipitate from solvent and form nuclei, which degree of polymerization is higher than the critical value. After that, these nuclei aggregate with each other, polymer nanoparticle or microparticle is formed. In the Fig.2, the schematic picture of agglomerated nanoparticles and grafted nanoparticles is shown.[24]

The function of stabilizer molecules is producing stabilizer grafted polystyrene-MTC copolymer molecules. In our experiment, we use polyvinyl

pyrrolidone (PVP) as stabilizer, a water-soluble polymer made from monomer N-vinylpyrrolidone. During polymerization, these molecules are adsorbed on the particle surface. Existence of stabilizer can stop the aggregate of nuclei. Depending on the amount of PVP in the reactor, and size of polymer particles can be controlled. Then nuclei grow by absorption of oligomeric radical from solvent and their polymerization with in the particles. Fig.3 shows schematic of the process of polystyrene synthesis.[25]

In this chapter, various sized polystyrene-MTC copolymer particles are synthesized in different conditions. Size of monodisperse polystyrene-MTC copolymer can be adjusted from 300nm to 3μm by controlling experiment parameters.

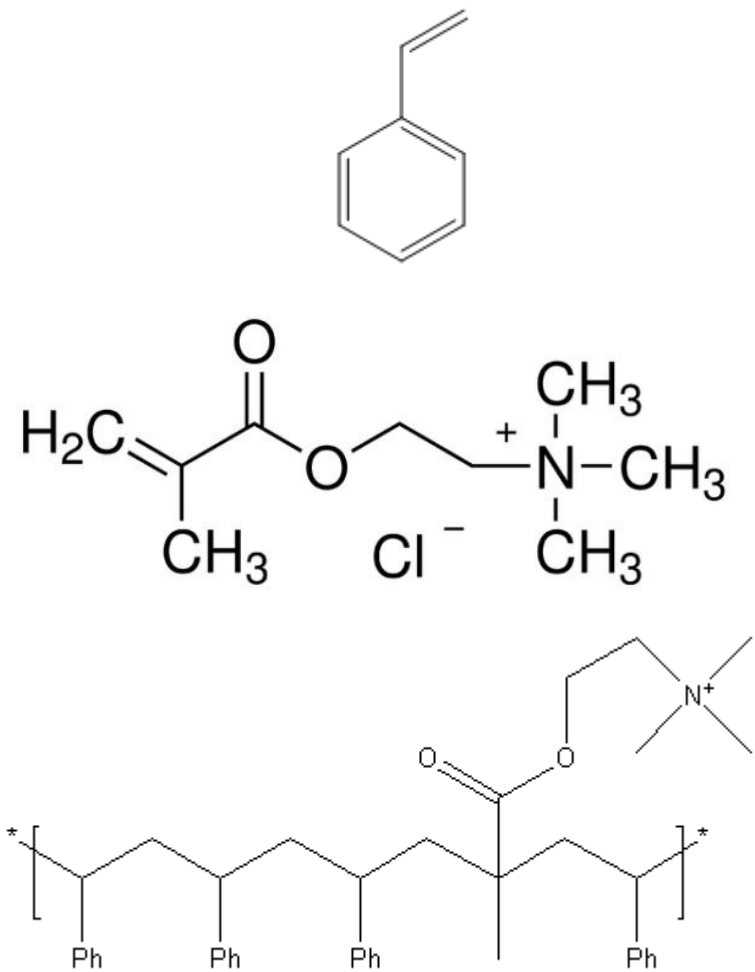

Figure 1 Molecular structure of styrene, MTC, and copolymer

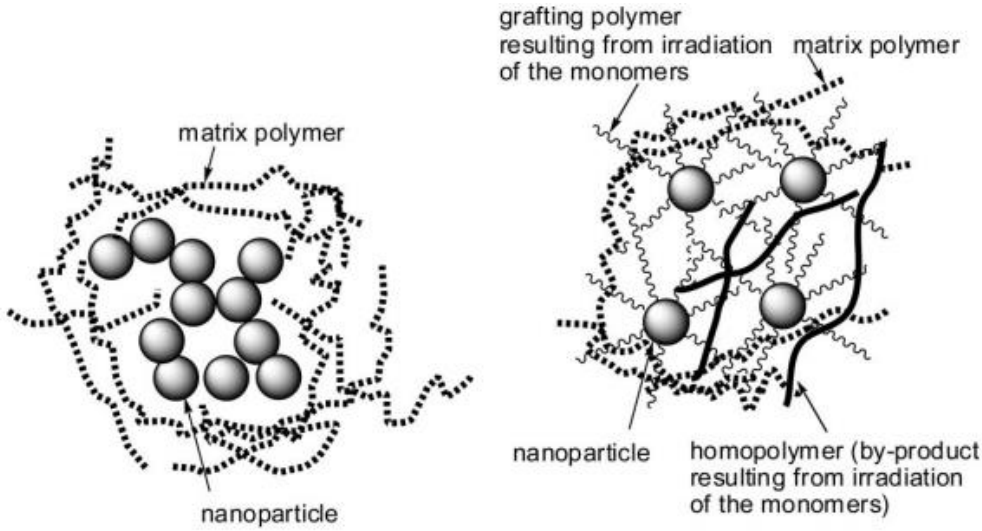

Figure 2 Schematic picture of agglomerated and grafted nanoparticles [24]

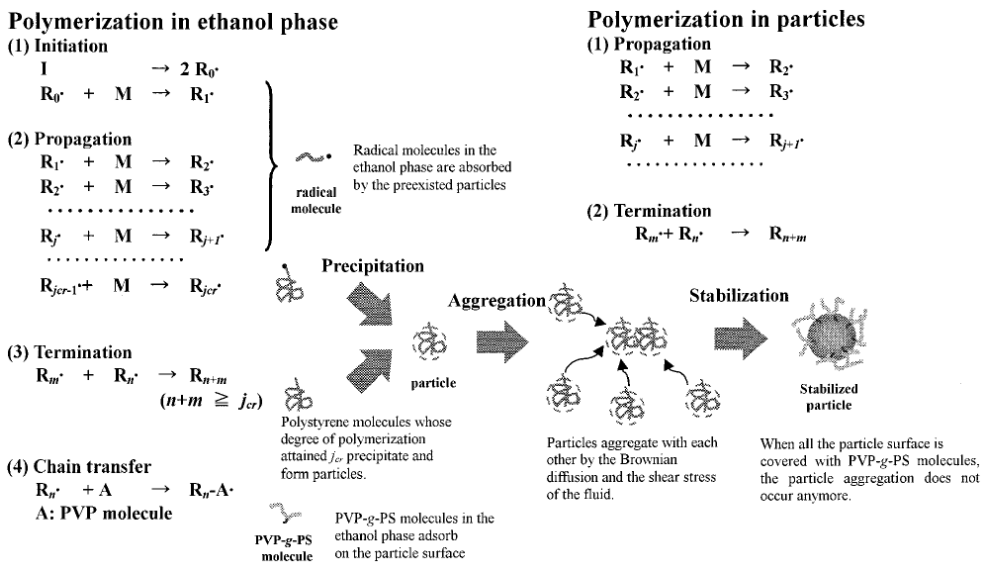

Figure 3 Schematic of the process of polystyrene synthesis. [25]

2.1.2 Synthesis of silica shell on the copolymer beads

Synthesis of core-shell particles with polymeric core and silica shell can be classified as one-step reaction [26~28] and two-step reaction [29~31]. In one-step method, one-pot synthesis is attractive in terms of simplicity due to no separation reactor and process between polymerization of core and silica shell coating. Wu et al.[26] reported synthesis of PS-silica core-shell particles by using MTC as co-monomer to increase the positive charge density on PS core, and then silica shell was coated on the core by electrostatic force between strong positive charged PS bead surface and negative charged hydrolysis production of tetraethyl orthosilicate (TEOS). Shim and his coworker synthesized silica-PS core-shell beads by using a positively charged silica sol and negative surface charged PS core.[27] They used an anionic initiator, potassium persulfate, and surface of PS core was modified to strong negative charge to increase attraction of positive charged silica sol. Armes et al. reported synthesis of silica-PS core-shell beads within a negative charged silica sol in the presence of a neutral initiator AIBN and an cationic initiator AIBA.[28] In two-step method, it includes a separation process of fabrication of polymeric core and coating silica shell. F.Caruso and his coworkers used a layer-by-layer method to coat silica shell on monodisperse polystyrene core with controllable shell thickness.[29] Different with layer-by-layer method, Xia, and his coworkers reported core-shell PS/silica beads synthesized by coating silica shell on -NH_2 grafted surface via the Stober method.[30] Wu et al. reported PS-SiO2 core-shell synthesized from positive charged PS beads under

at 70°C and an acid environment for a long reaction time.[31] However, these two-step methods generally have a relative complex fabrication procedure and long processing time due to the necessary of changing the reaction environment and surface modification of PS beads between reactions of polymerization of polystyrene core and coating silica shell.

In our experiment, monodisperse polystyrene-MTC core-shell beads are synthesized by using one-step reaction. Polystyrene-MTC beads with different size are synthesized by addition polymerization in 70°C. Then reactor is cooled down to 50°C to coat a silica shell by adding ammonia as catalyst and TEOS as silica sources. By adjusting amount of ammonia and TEOS, shell shows uniform distribution and smooth surface; also thickness of shell also can be controlled. Micron-sized core-shell beads can be easily synthesized by using AIBN as initiator and alcohol as solvent. But in the case of submicron sized particles, synthesis of submicron polymeric core needs strong polarity solution, like pure water. However, water is also catalyst of hydrolysis reaction of TEOS. Excess catalyst will cause the formation of tiny silica particles. Therefore, in the case for synthesis of submicron particles in week polarity solution, seeding process is necessary. Because of this extra seeding process, both submicron sized particles and micron sized particles can be synthesized.

2.2 Experiment and analysis

2.2.1 Materials

Styrene, TEOS, 2-(methacryloyl)ethyltrimethylammonium chloride (MTC), 2,2-Azobis(2-methylpropionitrile), ammonia 30% water solution, Polyvinylpyrrolidone (PVP) with both average molar masses of 40kg/mol and 360kg/mol were purchased from Sigma-Aldrich Co. (United States of America). 2-(azo(1-cyano-1-methylethyl))-2-methylpropane nitrile(AIBN), was purchased from J.T Baker Co. (United States of America). All materials above were used without further purification.

2.2.2 Synthesis of submicron polystyrene spheres

AIBN was used as initiator, PVP was used as stabilizer and styrene was used as monomer, MTC was used as co-monomer. Deionized water and ethanol were used as solvent. All of PVP, half of ethanol was charged into a 250 mL two-necked flask. After sealing one of the openings of two-necked flask by plug, reactor was deoxygenated by fluxing the nitrogen gas at room temperature for 10min. Meanwhile, solution was stirred by stirring bar, with a constant 300rpm. Then half of styrene was injected into reactor by injection syringe, which all of the AIBN was dissolved in it before injection. After 10 more minutes to remove all the oxygen in reactor, reaction temperature was gradually increased to 70°C on the hot plate. 1.5h later, after seeding process in first step, all of remaining styrene and ethanol and all of MTC and water were

added into two-necked flask by injection syringe. Then temperature was held at 70°C for polymerization of styrene and MTC. After polymerization for 20h, reactor was cooled naturally to 50°C to avoid further polymerization reaction during coating step. Following by adding ammonia and TEOS into reactor syringe for 1 hour, silica shell was coated on polymeric core. As-synthesize spheres were purified and separated from the other reaction solution by centrifuging at 11000rpm for 10min for 3 times, washed with pure ethanol. Temperature-time plot of the synthesis process of submicron particles is shown in Fig.4.

2.2.3 Synthesis of micron-sized polystyrene spheres

AIBN was used as initiator, PVP was used as stabilizer and styrene was used as monomer, MTC was used as co-monomer. Deionized water and ethanol were used as solvent. All of PVP, ethanol and water were charged into a 250 mL two-necked flask. After sealing one of the openings of two-necked flask by plug, reactor was deoxygenated by fluxing nitrogen gas at room temperature for 10min. Meanwhile, the solution was stirred by stirring bar, with a constant 300rpm. Then all of styrene and MTC was injected into reactor by injection syringe, which all of AIBN was dissolved in styrene before injection. After 10 more minutes to remove all oxygen in reactor, reaction temperature was gradually increased to 70°C on the hot plate. Then the temperature was held at 70°C for polymerization of styrene and MTC. After polymerization, reactor was cooled naturally to 50°C to avoid further polymerization reaction during

coating step. Following by adding ammonia and TEOS into reactor syringe for 1 hour, silica shell was coated on polymeric core. As-synthesize spheres were purified and separated from other reaction medium by centrifuging at 6000rpm for 10min for 3 times, washed with pure ethanol. Temperature-time plot of synthesis process of micron-sized particles is shown in Fig.5.

2.2.3 Analysis tools

The scanning electron microscopy (SEM) samples were prepared with gold or platinum coating to increase the conductivity. SEM images were obtained by Hitachi S4800 with operation voltage of 10~30kV.

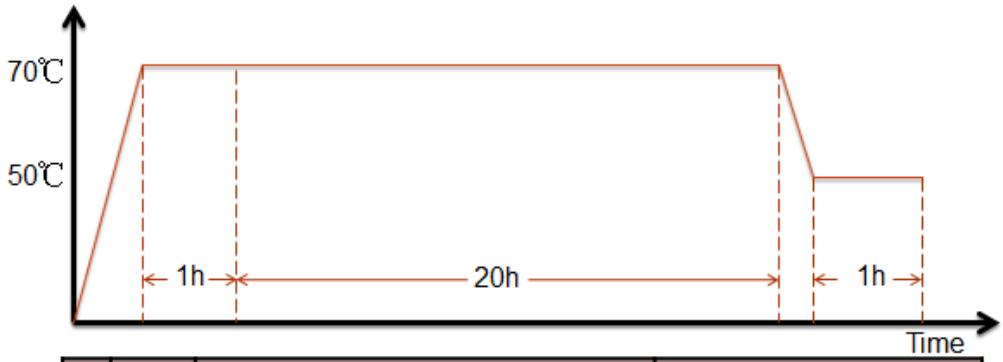

	Time	Additive reagent	Function
1	1 h	All of PVP AIBN Half of St EtOH	Seeding
2	20h	All of MTC H_2O Half of St EtOH	Polymerization of PS core
3	1h	NH_3 TEOS	Coating of silica shell

Figure 4 Schematic plot of the synthesis process of submicron particles

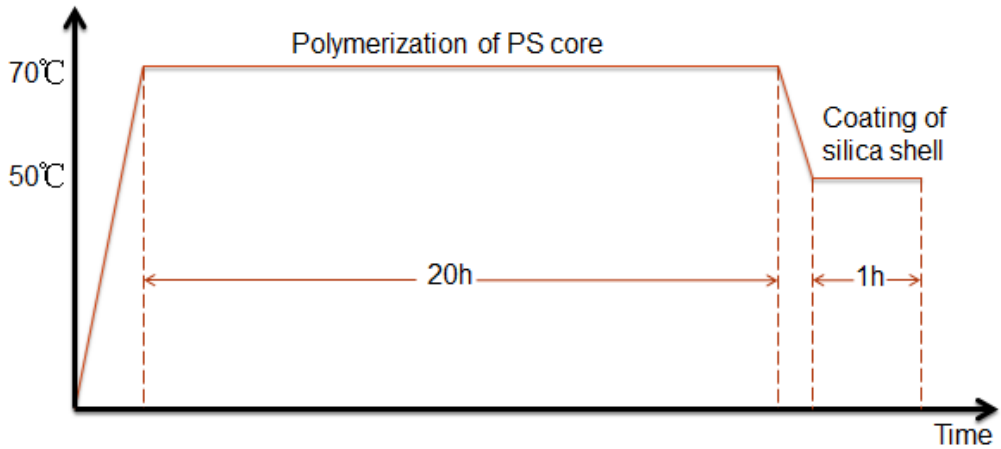

	Time	Additive reagent	Function
1	20h	PVP AIBN St MTC EtOH H_2O	Polymerization of PS core
2	1h	NH_3 TEOS	Coating of silica shell

Figure 5 Schematic plot of the synthesis process of micron-sized particles

2.3 Results and discussion

Because water is also a kind of weak lewis base, which works as catalyst of hydrolysis reaction of TEOS, existence of excess catalyst will cause formation of tiny silica particles instead of coating on PS core. In order to coat silica shell on polymeric core in one reactor, we have to avoid using pure water as solvent, so we choice and fix the mixture of 60mL ethanol and 5mL water as solvent to investigate the influence of other factors on size, morphology and distribution of PS-silica core-shell beads.

2.3.1 Synthesis of submicron core-shell spheres

In general, synthesis of submicron particles needs strong polarity solution like pure water, to reduce the solubility of PS nuclei to decrease size of polymeric particles. But water is also catalyst of hydrolysis reaction of TEOS, excess catalyst will cause formation of tiny silica particles. And also initiator AIBA, which is generally used in the synthesis of submicron polystyrene spheres have a very poor solubility in alcohol solvent. So in the case for synthesis of submicron particles in week polarity solution, a seeding process is necessary.

Effect of concentration of RPM on size and uniformity of core-shell beads

Because using monodisperse beads is a precondition of formation of HCP particle array. Meanwhile, size of silica shell is mainly determined by size of

polymeric core. The optimal condition of synthesis of monodisperse polystyrene-MTC core was investigated. In order to study effect of RPM on uniformity and size of polymeric core, RPM was selected as 150, 300, 360, and 450. Formulations used in this part of experiment were as follows: AIBN: 0.05g St: 12mL, MTC: 0.2mL, PVP: 1.5g, EtOH: 60mL, H_2O: 5mL.

Fig.6 shows SEM image of as-synthesized core-shell particles with different rpm, and the table of individual experiment condition and the relationship between the standard deviation of size and rpm. RPM is change from 150rpm to 450rpm.

Because different of RPM will cause different shear force in the reactor, if the shear force is too weak, the effect of stirring is also very weak. In this case, there is serious aggregation phenomenon of polymeric bead. In this case, instead of individual particles, a polymeric bulk is formed. On the other hand, high rpm will cause high shear force. If rpm is too high, strong eddy current will also reduce uniformity of particles. By these reasons, a moderate rpm is necessary. According to SEM image, we select 360rpm as optimal condition in the following experiment.

Effect of concentration of initiator (AIBN) on size and uniformity of core-shell sphere

In order to investigate effect of initiator concentration on uniformity and size of core-shell spheres, amount of AIBN was selected as 0.05g, 0.1g, 0.2g

and 0.3g. Formulations used in this part of experiment were as follows: St: 12mL, MTC: 0.2mL, PVP: 1.5g, EtOH: 60mL, H_2O: 5mL, TEOS: 6mL, ammonia: 4mL. RPM: 360

Fig.7 shows SEM image of as-synthesized core-shell particles with different amount of initiator and table of individual experiment condition and relationship between size of core-shell beads and amount of imitator. Amount of AIBN is changed from 0.05g to 0.3g.

In general, as concentration of initiator increases, size of particles should reduce by seeding effect, more nuclei are formed in the polymerization.[32] But in our experiment, size of core-shell beads increases with increasing of concentration of AIBN. This can be explained by following reasons. At first, more seeds are produced with lower molecular weight than general cases. Then stabilizer grafted polymeric core becomes more soluble and stabilizer becomes less effective. As a result, size of polymeric core is able to grow bigger.[33,34] Therefore, we can conclude that, by increasing amount of AIBN, size of the core-shell beads become bigger.

Effect of concentration of styrene (monomer) on size and uniformity of core-shell beads

In order to investigate effect of styrene on uniformity and size of core-shell beads, amount of AIBN was selected as 8mL, 10mL, 12mL, and 14mL. Formulations used in this part of experiment were as follows: AIBN:

0.05g, MTC: 0.2mL, PVP: 1.5g, EtOH: 60mL, H_2O: 5mL, TEOS: 6mL, ammonia: 4mL. RPM: 360.

Fig.8 shows SEM image of as-synthesized core-shell particles with different amount of monomer and table of individual experiment condition and relationship between size of core-shell beads and amount of imitator. Amount of AIBN is changed from 8mL to 14mL.

In general, as increasing of amount of monomer in reaction, size of polymeric core should reduce, because of seeding effect.[32] But precondition of this conclusion is that monomer dissolves well in solvent to produce more radicals. In the case of our experiment, solvent is mixture of water and ethanol. As a polar solvent, both of them do not have a good solubility for styrene. So, instead of mixture of water and ethanol, as a non-polar solvent, styrene works as actual solvent for polystyrene oligomer. By this reason, more amount of styrene increases solubility of polystyrene oligomer. The precipitation of polymeric oligomers becomes difficult; this effect increases the critical degree of polymerization in the reaction.[33] So we can conclude that, by increasing amount of monomer, the size of the core-shell beads become bigger.

Effect of concentration of PVP (stabilizer) on size and uniformity of core-shell beads

In order to investigate effect of PVP on uniformity and size of core-shell beads, amount of AIBN was selected as 1g, 1.25g, 1.5g and 1.75g. Formulations

used in this part of experiment were as follows: AIBN: 0.05g, St: 12ml, MTC: 0.2mL, EtOH: 60mL, H_2O: 5mL, TEOS: 6mL, ammonia: 4mL. Rpm: 360.

Fig.9 shows SEM image of as-synthesized core-shell particles with different amount of stabilizer and table of individual experiment condition and relationship between size of core-shell beads and amount of imitator. amount of PVP is changed from 1g to 1.75g.

SEM image shows that size of core-shell beads decrease with increasing of amount of PVP in reaction. This phenomenon can be explained as follow. More amount of PVP in solvent can increase amount of PVP which absorbed by individual polymeric oligomers. Because PVP grafted polymeric core is keeping on absorbing onto the growing beads until particles is stable enough to avoid further coalescence by protection of PVP graft.[33,34] So we can conclude that, by increasing amount of stabilizer, size of core-shell beads become smaller.

Effect of concentration of MTC (co-monomer) on size and uniformity of core-shell beads

In order to investigate effect of MTC on uniformity and size of core-shell beads, amount of AIBN was selected as 0mL, 0.2mL, 0.3mL and 0.4mL. Formulations used in this part of experiment were as follows: AIBN: 0.05g, St: 12ml, PVP: 1.5g, EtOH: 60mL, H_2O: 5mL, TEOS: 6mL, ammonia: 4mL. RPM: 360.

Fig.10 shows SEM image of as-synthesized core-shell particles with different amount of MTC, and table of individual experiment condition and relationship between size of core-shell beads and amount of imitator. Amount of MTC is changed from 0mL to 0.4mL

Main function of MTC is increasing positive charge density on polymeric core surface. SEM image shows that, silica shell is not able to be coated on polymeric core without MTC. This is caused by low positive charge density on polymeric core surface, so the attractive force of polymeric core to TEOS or hydrolyzed TEOS is too weak to absorb silica on the surface. Instead of form a uniform silica shell, tiny silica beads are produced.

On the other hand, with increasing of amount of MTC, size of core-shell beads become bigger. I think this result is caused by following reasons. Because comparing with amount of other monomer (styrene) in the experiment, amount of MTC is relative small. Different with changing amount of monomer, various amount of MTC will not change amount of non-polar solvent in reaction too much. There are two main affection factors of MTC on the size of core-shell particles. First one is the steric-hinerance effect. Because of relative big molecule of MTC, it will reduce effect of stabilizer. In other word, increasing amount of MTC increases size of polymeric core. Other factor is electrostatic effect. More amount of MTC increases positive charge density on the surface, that is, thicker silica shell can be adsorbed on the polymeric core. But if positive charge density of polymeric core is too high, it will cause a lot tiny nuclei on the silica shell. In this case, silica shell is not a smooth surface

any more, but a rough surface with a lot of protuberances. To conclude, existence of MTC is necessary to coat silica shell on the polymeric core, by increasing amount of MTC, size of core-shell beads become bigger.

2.3.2 Synthesis of micron-sized core-shell spheres

In the case of synthesis of micron-sized core-shell beads, all the experiment process were same with synthesis of submicron core-shell beads, with exception of the absent of seeding step. So all factors which affected size and uniformity of core-shell beads had same tendency with previous experiment, and needed not to be repeated here. Fig.11 shows the as-synthesis micron-sized core-shell spheres and the recipe of experiment.

2.3.3 Features of as-synthesized particles

There are two important features of as-synthesized particles, one is shrinkable shell, and another is decomposable core.

Shrinkage shell is caused by weak base environment in the reactor. As a weak base, ammonia can not only work as catalyst of the hydroxylation of TEOS, but also it can increase the porosity of coated silica shell. Because of porous silica shell, during thermal treatment, size of the hollow silica beads becomes smaller.

Decomposable core is caused by the common property of organic core. Polymeric core cannot survive at high temperature in the air. In the case for polystyrene, if temperature is higher than 550°C, it will completely decompose

from solid state to gas state in the atmosphere. According to these two unique properties of as-synthesized core-shell particles, after thermal treatment at high temperature in the air, size of hollow silica beads become smaller, meantime, PS core is removed and spherical shape is remained. Core-shell particle is transformed into hollow silica shell with a smaller size than as-synthesized beads. Fig.12 shows the schematic picture of features of as-synthesized particles.

SEM images of core-shell particles synthesized with different amount of TEOS after thermal treatment are shown in Fig.13. As we know that if we increase amount of TEOS in the reaction, thickness of silica shell will become thicker. During high temperature thermal treatment, if silica shell is not thick enough, hollow particle will not able to maintain spherical shape. However, on the other hand, more tiny silica beads are formed by using more TEOS due to more amount of silicon sources.

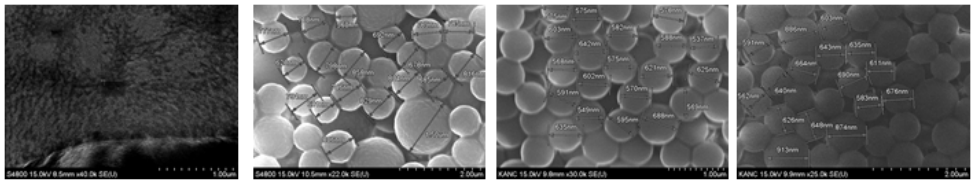

1 2 3 4

	PVP	AIBN	EtOH	H_2O	St	MTC	Time	RPM	Size	Deviation
1	1.5g	0.05g	60mL	5mL	12mL	0.2mL	22h	150	/	/
2	1.5g	0.05g	60mL	5mL	12mL	0.2mL	22h	300	770nm	188nm
3	1.5g	0.05g	60mL	5mL	12mL	0.2mL	22h	360	589nm	29nm
4	1.5g	0.05g	60mL	5mL	12mL	0.2mL	22h	450	674nm	111nm

Figure 6 SEM images of polystyrene-MTC copolymer beads at various RPM

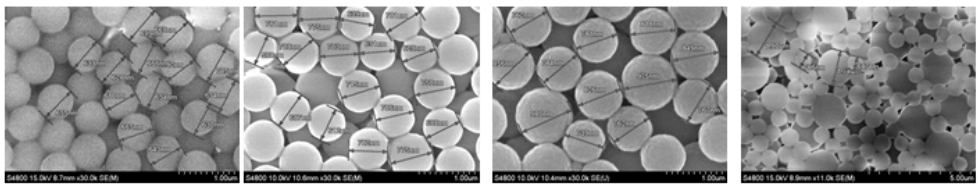

1 2 3 4

	PVP	AIBN	EtOH	H_2O	St	MTC	Time	RPM	Size	Deviation
1	1.5g	0.05g	60mL	5mL	12mL	0.2mL	22h	360	654nm	26nm
2	1.5g	0.1g	60mL	5mL	12mL	0.2mL	22h	360	690nm	56nm
3	1.5g	0.2g	60mL	5mL	12mL	0.2mL	22h	360	830nm	82nm
4	1.5g	0.3g	60mL	5mL	12mL	0.2mL	22h	360	/	/

TEOS: 6mL NH_3: 4mL

Figure 7 SEM images of polystyrene-MTC core-shell beads at various amount of AIBN

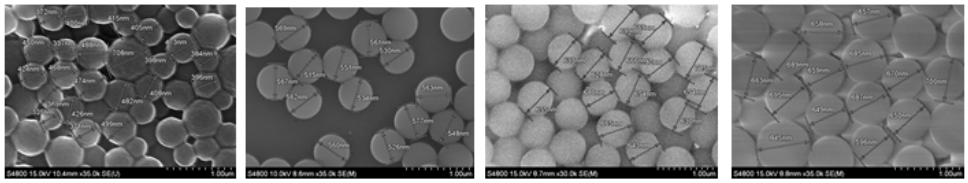

1 2 3 4

	PVP	AIBN	EtOH	H_2O	St	MTC	Time	RPM	Size	Deviation
1	1.5g	0.05g	60mL	5mL	8mL	0.2mL	22h	360	550nm	19nm
2	1.5g	0.05g	60mL	5mL	10mL	0.2mL	22h	360	630nm	26nm
3	1.5g	0.05g	60mL	5mL	12mL	0.2mL	22h	360	654nm	26nm
4	1.5g	0.05g	60mL	5mL	14mL	0.2mL	22h	360	690nm	50nm

TEOS: 6mL NH_3: 4mL

Figure 8 SEM images of polystyrene-MTC core-shell beads at various amount of styrene

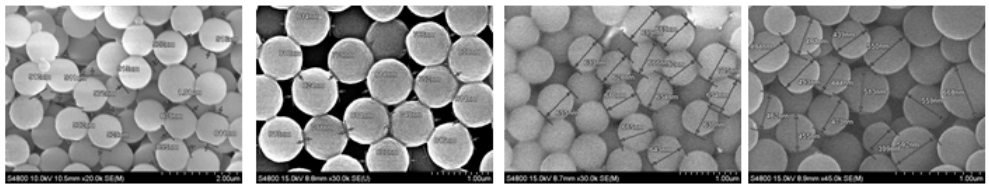

1 2 3 4

	PVP	AIBN	EtOH	H_2O	St	MTC	Time	RPM	Size	Deviation
1	1.0g	0.05g	60mL	5mL	12mL	0.2mL	22h	360	921nm	42nm
2	1.25g	0.05g	60mL	5mL	12mL	0.2mL	22h	360	800nm	30nm
3	1.5g	0.05g	60mL	5mL	12mL	0.2mL	22h	360	654nm	26nm
4	1.75g	0.05g	60mL	5mL	12mL	0.2mL	22h	360	508nm	71nm

TEOS: 6mL NH_3: 4mL

Figure 9 SEM images of polystyrene-MTC core-shell beads at various amount of PVP

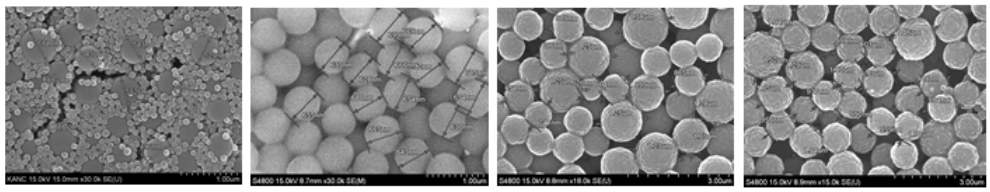

1 2 3 4

	PVP	AIBN	EtOH	H_2O	St	MTC	Time	RPM	Size	Deviation
1	1.5g	0.05g	60mL	5mL	12mL	0mL	22h	360	/	/
2	1.5g	0.05g	60mL	5mL	12mL	0.2mL	22h	360	654nm	26nm
3	1.5g	0.05g	60mL	5mL	12mL	0.3mL	22h	360	/	/
4	1.5g	0.05g	60mL	5mL	12mL	0.4mL	22h	360	/	/

TEOS: 6mL NH_3: 4mL

Figure 10 SEM images of polystyrene-MTC core-shell beads at various amount of MTC

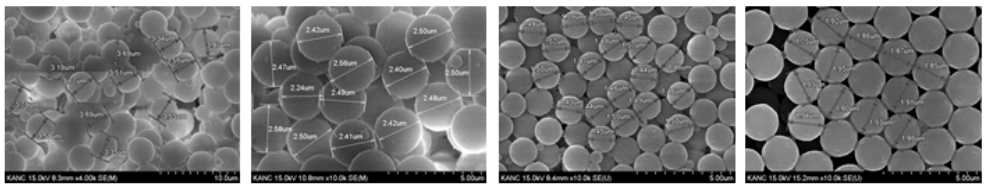

	PVP	AIBN	St	MTC	NH_3	TEOS	EtOH	H_2O	Size	Deviation
1	1.5g	0.2g	12mL	0.4mL	4mL	6mL	60mL	5mL	3594nm	181nm
2	1.5g	0.2g	12mL	0.2mL	4mL	6mL	60mL	5mL	2477nm	55nm
3	1g	0.1g	12mL	0.2mL	4mL	6mL	60mL	5mL	1880nm	61nm
4	1.5g	0.1g	12mL	0.2mL	4mL	6mL	60mL	5mL	1460nm	32nm

Black PVP: molecular weight 40,000 **Blue PVP: molecular weight 360,000**

Figure 11 SEM images of submicron sized polystyrene-MTC core-shell beads

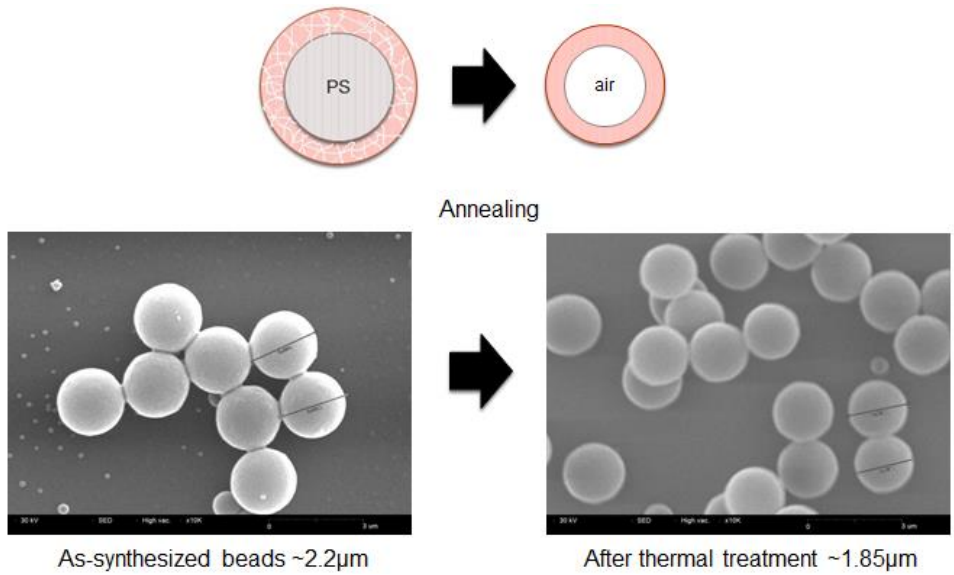

Figure 12 SEM image and schematic picture of shrinkable feature of as-synthesized particles

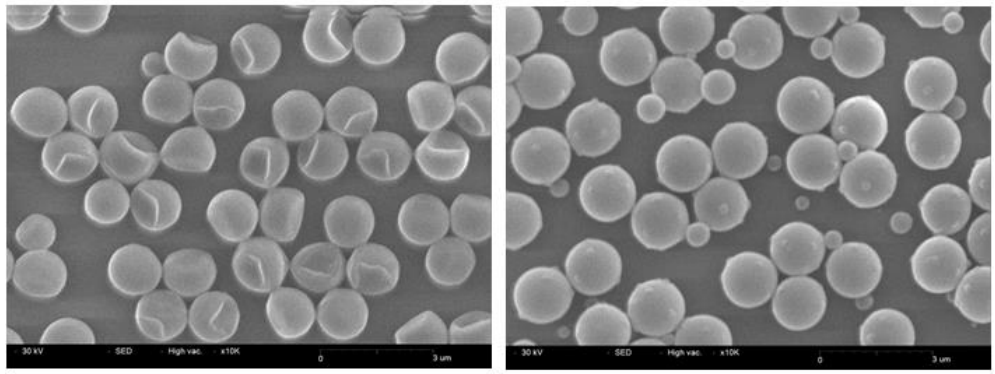

6 mL TEOS 12mL TEOS

Figure 13 SEM images of core-shell particles synthesized with different amount of TEOS after thermal treatment

2.4 Conclusion

In this chapter, various sized monodisperse shrinkable PS-silica core-shell beads was synthesized. By adjusting different experiment parameter, size of core-shell beads could be synthesized from 300nm to 3μm. Effects on the uniformity and size of RPM, amount of initiator, stabilizer, monomer, and co-monomer were investigated. Uniform polystyrene-MTC core was successfully synthesized and smooth silica shell is coated on the core.

There were two important features of as-synthesized particles, one was shrinkable shell, and another was decomposable core. After thermal treatment at high temperature in the air, size of silica shell became smaller, meantime, PS core was removed and spherical shape is remained. Core-shell particle was transformed into hollow silica shell with a smaller size than as-synthesized beads.

Chapter 3. Fabrication of hexagonal non-closed packed hollow silica particle on sapphire substrate

3.1 Introduction

Colloidal crystal made by inorganic or polymer particles attracted extensive interest due to their promising potential application, such as optical, photonic bandgap materials, data storage nanoparticle lithography and sensing [35~37]. A lot of technologies have been researched to fabricate large-area 2D colloidal crystal, such as spin-coating method [38], electric-field-induced eletrokinetic flowing [39], air–water interfacial floating method [40], and Lamgmuir-Blodgett deposition [41]. Comparing with close-packed colloidal crystal, non-close-packed (NCP) colloidal crystals have a tunable distance between individual particles. This unique property makes them to be very attractive materials for photonic devices. Until now, monolayer NCP colloidal crystal has been fabricated by the several different methods, such as reactive ion etching, template-induced assembly, optical tweezers, soft lithography, and manipulation of dipole-dipole interaction.[42~46] However, all of these methods have relative complicated fabrication process or very small area of NCP monolayer.

In our research, a novel and simple method of fabrication of hexagonal non-closed packed hollow silica particle on sapphire substrate was proposed. The main point in this study was using shrinkable property of PS-silica

core-shell beads. At first, hexagonal closed packed PS-silica core-shell beads was coated on the sapphire substrate by spin-coating method. Then substrate was heated in the furnace at high temperature to remove organic core and reduce size of silica shell. After thermal treatment, HCP PS-silica core-shell beads array was transformed to HNCP hollow silica particle array. By controlling time of thermal treatment, coverage percentage of hollow silica beads on the substrate was changed from 85% to 50%. However, due to connection between neighboring particles, HNCP pattern was not perfect. These connection defects were inevitably formed during thermal treatment with low ramping time. The schematic picture and SEM image of this fabrication process is shown in Fig.14.

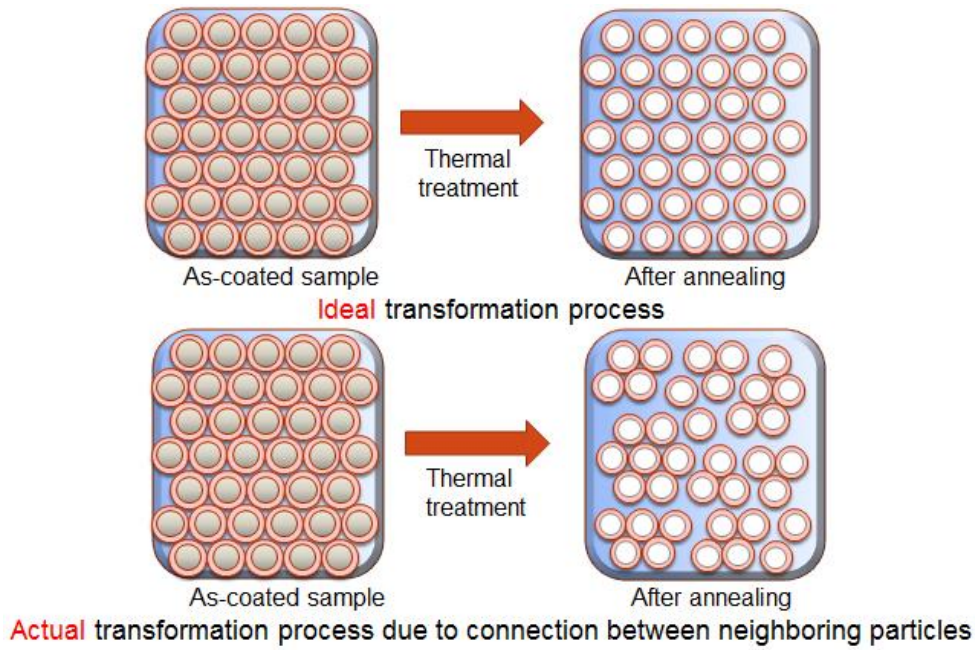

Figure 14 Schematic picture and SEM image of transformation from HCP array to HNCP array

3.2 Experiment and analysis

3.2.1 Materials

Ethanol, sulfuric acid and hydrogen peroxide were purchased from J.T. Baker Co. (USA). PS-silica core-shell beads were synthesized by previous method and dispersed in ethanol solvent. All of materials were used without further purification.

3.2.2 Fabrication of HCP monolayer of core-shell beads by spin-coating

Because sapphire substrate is hydrophobic surface, substrates were treated in the piranha solution (3:1 v/v, 98% sulfuric acid and 35% hydrogen peroxide) at room temperature for 30min to modify surface of substrate from hydrophobic to hydrophilic. Piranha solution could break Al-O bonding and modify surface to hydroxyl group on it. After surface treatment, sapphire substrate was washed by copious amount of deionized water, and stored in the deionized water until use.

There were several steps in spin-coating experiment. First one was cleaning; several drop of deionized water was dropped on sapphire substrate, and dried by the rotation of spin-coater machine at 4000rpm for 10s, repeat for three times. Then core-shell beads solution was dropped on the substrate, and then particle solution was whipped by pipet carefully to separate solution to whole substrate uniformly. After that, spin-coater machine was turned on;

solvent was evaporated under high rotation speed condition. In the end, as-coated substrate was stored in the petri dish until following experiment.

3.2.3 Fabrication of HNCP monolayer of hollow silica beads by thermal treatment

As-coated sapphire substrates with HCP monolayer core-shell particle were annealed in furnace at 1100°C under air atmosphere for certain time. After thermal treatment at high temperature in the air, size of hollow silica beads became smaller, meantime, PS core was removed. Core-shell particle was transformed into hollow silica shell with a smaller size than as-synthesized beads.

3.2.4 Analysis tools

Scanning electron microscopy (SEM) samples were prepared with gold or platinum coating to increase conductivity. SEM images were obtained by Hitachi S4800 with operation voltage of 10~30kV.

3.3 Results and discuss

3.2.1 Fabrication of HCP monolayer of core-shell beads by spin-coating

Spin-coating methods have an advantage for both scaling-up and mass production. It is the most suitable method for industry production, but it is also very difficult to find optimal window to fabricate HCP monolayer of colloidal crystal due to the sensitivity of experiment parameters and environment conditions.

The capillary force is main driving force for formation of HCP particle array. The mechanism of formation of monolayer by using spin-coating methods is balance between evaporation of solvent and capillary force between particles.[47] Capillary force is caused by difference in gas phase evaporation rate and surface force effect caused by varied liquid surface contact line originated by hydrostatic pressure.[48] Capillary forces take effect when height of liquid is about or lower than diameter of particles. Evaporation of solvent and centrifuge force is caused by high rotation speed condition of spin-coater machine. Balance between these three factors is the key point of fabrication of HCP monolayer particles. For example, by adjusting rpm, we can control rate of solvent evaporation and centrifuge forces. If rpm is too high in the spin-coating process, high centrifuge forces and high evaporation rate will cause low coverage due to imbalance between capillary force and centrifuge force, capillary force is not strong enough to hold particles together. On the

other hand, if rpm is too low, low centrifuge force and low evaporation rate will cause thick fluid thickness and capillary forces is to stronger than centrifuge force. In this case, multilayer is formed due to unbalance of these forces. Only when experiment parameters are very precisely controlled, monolayer of particles can be coated on the substrate uniformly. The process of spin coating of particles was shown is Fig.15.

General spin-coating process concludes following four steps , first stage is deposition of coating fluid onto the wafer or substrate, usually this dispense stage provides a substantial excess of coating solution compared to amount that will ultimately be required in the final coating thickness. During the later stage, a uniform thin film of fluid will be formed by balance of centrifuge force and shearing force. Excess solution will be rotated out of film. At final stage, because of high rotation speed, evaporation of solvent will be accelerated. Fig.15 shows schematic picture of spin-coating process.

In the spin-coating experiment, a lot of parameter will influence coating quality of sample, such as RPM, spin time, acceleration for each spin step, solvent, concentration and size of particles, temperature and humidity of atmosphere. All of these parameters are very important factors to determine quality of coated sample. According to the conclusion of other papers,[47,49] the function of each factor and reasonable design are summarized in the Table.1.

By adjusting all of these factors, optimal condition is found. SEM images of coated sample shows that core-shell beads are coated on the 2-inch sized

sapphire substrate and HCP monolayer is dominated structure in whole substrate. Fig.16 shows the SEM image of coated sample from region to region on 2-inch sized sapphire substrate.

3.3.3 Fabrication of HNCP monolayer of hollow silica beads by thermal treatment

There are two important features of as-synthesized particles, one is shrinkable shell, and another is decomposable core. During thermal treatment in furnace, polymeric core cannot survive in high temperature; it will completely decompose from solid state to gas state in the atmosphere. Meantime, because of porous silica shell, size of hollow silica beads becomes smaller during process of thermal treatment. According to these two unique properties of as-synthesized core-shell particles, after thermal treatment at high temperature in the air, size of hollow silica beads become smaller, meantime, PS core is removed and spherical shape is remained. Core-shell particle is transformed into hollow silica shell with a smaller size than as-synthesized beads.

In this study, temperature is set as 1100°C, not only for transformation of HNCP patterning, but also for fixing hollow shell tightly on the sapphire substrate by necking effect. As increasing of heating time, silica shell becomes more and more condense, which means size of silica shell becomes smaller and smaller. Depending on thermal treatment time, coverage percentage can be adjusted from 85% to 50%. According to these SEM images we can know

that, size of hollow shell decreases with longer heating time. PS-silica core-shell beads can shrink into a hollow silica shell with 55% size of as-synthesized particles at a minimum. Fig.17 shows the SEM image of NCP silica shell coated on sapphire substrate with different thermal treatment time. Fig.18 shows the dependence of thermal treatment time and coverage percentage of hollow silica shell on the sapphire substrate after thermal treatment.

Main defects in HNCP silica hollow particle pattern is connection between particles. Formation of this defect can be explained as follow. Due to porosity of silica shell, a contraction force is formed at high temperature. This force points to the center of silica shell. It is also driving force of formation of fully isolated HNCP array. But there is also other attraction force between neighboring particles, which connect neighboring particle with each other. This necking between hollow silica shells is formed at high temperature. Connection prevents formation of fully isolated individual particles. Fig.19 shows the schematic picture of these two forces. Due to connection between neighboring particles, HNCP pattern is not perfect. These connection defects are inevitably formed during thermal treatment with low ramping time (3°C/min in the furnace). However in the case of thermal treatment with high ramping time, like in MOCVD camber (180°C/min), connection between neighboring particles can be avoided.

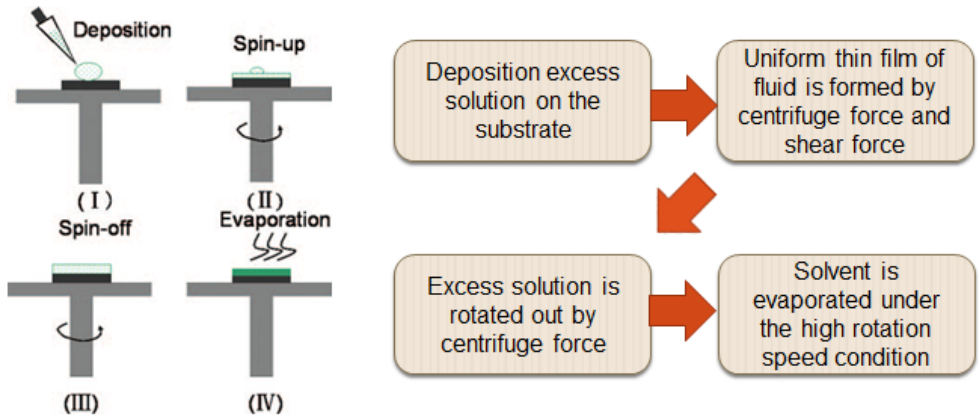

Figure 15 Schematic picture of spin coating process

Main factors	Reasonable design
Spin step	Bigger sized, worse wettability substrate needs more step
RPM1	Balance between evaporation and centrifuge forces (most important)
RPM2	Dry the substrate, remove multilayer on the edge
Acceleration	As high as possible
Solvent	Consider wettability and evaporation rate
Concentration & size of particles	Depending on different size, concentration of solute need to be adjusted

	RPM1	T1	RPM2	T2	Size of silica	RAMP	Concentration	Solution	Size of substrate
1	100rpm	5s	4000rpm	10s	1440nm	4s	15%	Ethanol	2 inch

Table 1 Function of each factor in the spin coating process and reasonable design

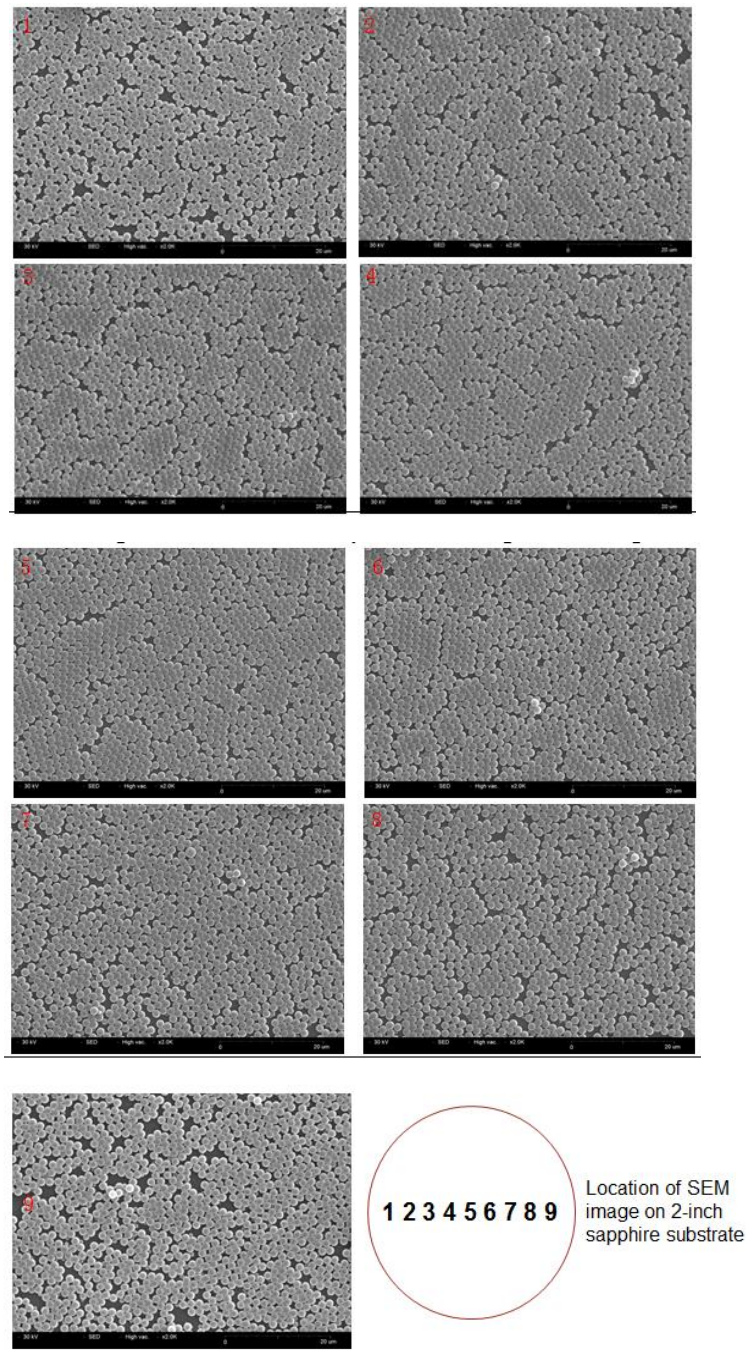

Figure 16 SEM image of coated sample from region to region on 2-inch sized sapphire substrate

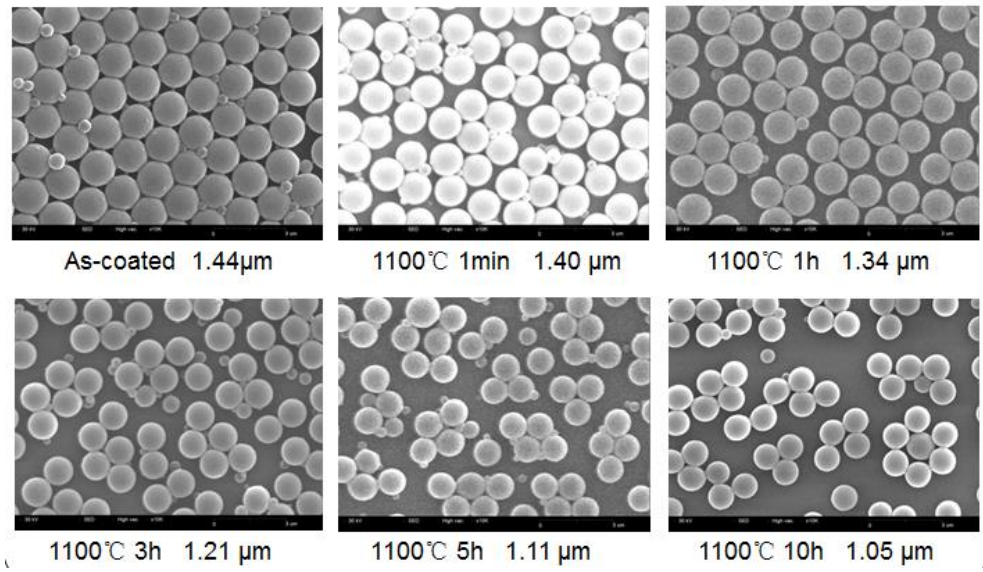

Figure 17 SEM image of NCP silica shell coated on sapphire substrate with different thermal treatment time

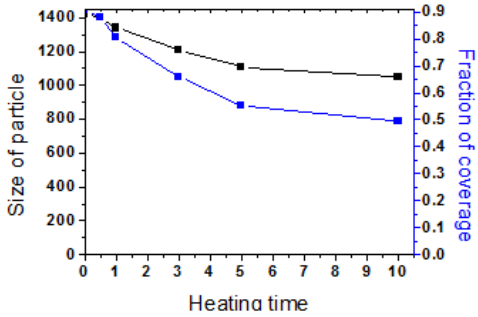

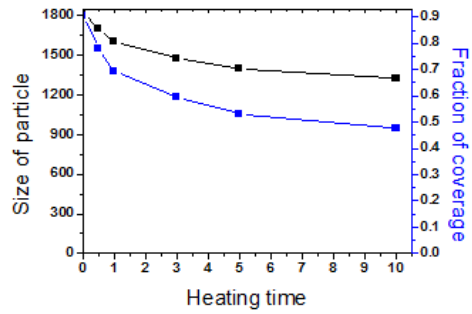

	PVP	AIBN	St	MTC	NH_3	TEOS	EtOH	H_2O	Size
1	1g	0.2g	12mL	0.2mL	6mL	12mL	60mL	5mL	1440nm
2	0.75g	0.2g	12mL	0.2mL	6mL	12mL	60mL	5mL	1830nm

Figure 18 Dependence of thermal treatment time and coverage percentage of hollow silica shell on the sapphire substrate after thermal treatment

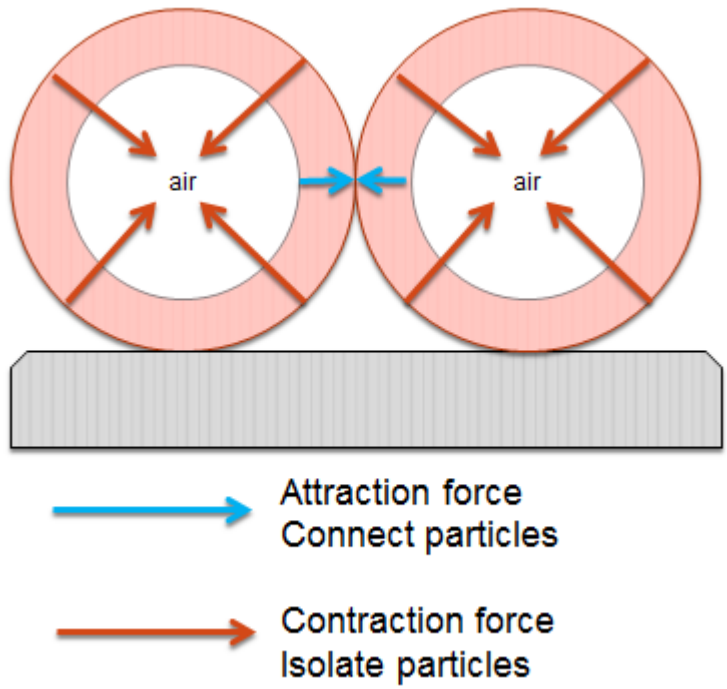

Figure 19 Schematic picture of formation of defects during thermal treatment

3.4 Conclusion

By adjusting several experiment parameters in spin-coating process, sapphire substrate coated by monolayer core-shell particles with HCP structure was fabricated successfully. SEM images from region to region showed that HCP monolayer was dominating in whole samples.

After thermal treatment, HCP core-shell particles array was transformed to HNCP hollow silica particles array. Depending on thermal treatment time, coverage percentage could be adjusted from 85% to 50%. According to these SEM images we can know that, size of hollow shell decreased with longer heating time. PS-silica core-shell beads could shrink into a hollow silica shell with 55% size of as-synthesized particles at a minimum.

Main defects in HNCP silica hollow particle pattern was connection between particles. Due to connection between neighboring particles, HNCP pattern was not perfect. These connection defects were inevitably formed during thermal treatment with low ramping time. However in the case of thermal treatment with high ramping time, like in MOCVD camber, connection between neighboring particles could be avoided.

Chapter 4. Growth GaN thin films on patterned sapphire substrate

4.1 Introduction

In the case of growth of GaN, homoepitaxy is a very difficult and high cost work due to the hardship of fabrication of GaN substrate. Although using the heteroepitaxial growth to fabricate GaN thin films solve problem of high cost in the fabrication process, the performance of devices are still suffered by poor crystal quality of GaN epitaxial layer. There are 3 main problems of heteroepitaxial layer. First problems the high threading dislocation density in the GaN thin films. Second problem is low external extraction efficiency of GaN based Led devices. Third problem is water bowing. Due to large difference of thermal expansion coefficient between sapphire substrate and GaN epitaxial layer, after growth at high temperature, bowing of water happens at room temperature. It will increase cost and lower quality of production.

In order to solve these problems of conventional GaN based LED devices, a lot of effective methods were proposed. One of the most famous methods is named as LEO. However, due to the complicated fabrication process, cost of this technique is quiet high. Other well-known method to fabricate high efficiency LED devices is PSS. This method is also very complicated and expensive. Recently, using silicon substrate or sapphire substrate coated by monolayer of silica beads as core to grow high quality GaN thin films was

reported. Existence of silica beads can not only work as mask to reduce dislocation density, but also increase external quantum efficiency and bowing effect. In order to further remove stress of GaN epitaxial film, one of seniors in our group, Jonghak Kim reported a method of using hollow silica monolayer coated sapphire as substrate to grow GaN thin films. Experiment result showed that stress of epitaxial films is greatly reduced.

In this work, HNCP hollow silica shell coated sapphire was used as substrate to growth GaN thin films. There are three advantages of patterning substrate. At first, hollow silica shell works as mask to reduce density of threading dislocations. Then, hollow silica shell can provide space to reduce stress of epitaxial layer. In the end, this periodic hollow particle array can increase external quantum efficiency by scattering effect.

4.2 Experiment and analysis

4.2.1 MOCVD system

In this work, Tomas Swan 3*2''(incorporated 3 substrates of 2 inch size) close coupled showerhead MOCVD system was used to grow GaN thin films. Solkatronics Blue-ammonia(NH_3) of 6N purity was used as nitrogen sources, and trimethylgallium (TMGa) was used as gallium sources.

4.2.2 Growth procedure

At first, HNCP hollow shell coated sample was heated at 1100°C for 5min as thermal cleaning in the MOCVD chamber. Then temperature of reactor was cooled down to 550°C to grow a low temperature GaN buffer layer at 100 Torr. Subsequently, temperature of reactor was heated to 1040°C for growth of GaN thin films.

4.2.3 Analysis tools

Scanning electron microscopy (SEM)

Scanning electron microscopy (SEM) samples were prepared with gold or platinum coating to increase the conductivity. SEM images were obtained by Hitachi S4800 with operation voltage of 10~30kV.

Photoluminescene (PL)

PL measurement was carried out at room temperature with 325nm line of He-Cd laser. The PL signal was disperse by a SPEX monochromator and detected by liquid-nitrogen-cooled charge couple device detector.

X-ray diffraction (XRD)

Panalytical X'pert instrument was used for high resolution XRD measurement and theta-2theta scan. The angle divergence of 12 arcsec or less can be obtained by 4 bounce Ge 022 channel cut monochromator.

4.3 Results and discuss

In the following experiment, HNCP hollow silica shell coated sapphire is used as substrate to grow GaN thin films. Size of particles before thermal treatment and after thermal treatment is 1.44μm and 1.33μm respectively. Coverage percentage of silica shell is about 80%, a very high value. GaN crystal can be grown from opening space on the substrate which comes from shrinkage of silica shell and the vacancy between closed packed particles. Width of space is about 200~400nm. In order to study the initial growth mode of GaN crystal, high temperature grow time is set as 3min. According to SEM image, we can know that all of GaN seeds located on the sapphire substrate between silica hollow shells. With more growth time, GaN are grown from isolated seeds into connective islands. Fig.20 shows SEM images of nucleation process of GaN thin films (3 min growth). Fig.21 shows SEM images of initial growth mode of GaN thin films (20min growth)

The buffer layer is essential to grow high quality of GaN thin films to avoid formation of polycrystalline GaN thin films. Buffer layer is polycrystalline GaN grown at low temperature. At high temperature, this buffer layer is recrystallized and transformed to crystalline GaN seed. Due to extra high coverage percentage of our substrate, a two-step method is selected to grow GaN thin films. After grown of buffer layer, MOCVD chamber was heated to high temperature to grow single crystalline GaN thin films. In general high pressure in MOCVD camber (300Tor.) is benefit from higher crystalline quality, but less tendency of lateral growth. On the other hand, low pressure is good

for increasing tendency of lateral overgrowth, but poorer crystal quality. Because of high coverage percentage of our substrate, we use high pressure growth for 30min, then low pressure growth for 2 hours. The reason of using high pressure growth for initial 30min is making a high quality GaN islands at first. Then using low pressure to coalesce these islands, crystal quality is expected higher than using low pressure mode only due to high-quality seeds. The cross section and plan view SEM images is shown is Fig.22. Due to high coverage percentage of substrate, GaN film is not fully coalescent. Reasons of this morphology are shown as follow. At first high coverage leaves less space for nucleation of GaN seed, then formation of films will become more difficult. Second factor is due to uniformity of films is not good enough. Existence of bilayer region or aggregate particles will also prevent both nucleation of GaN and lateral over growth. Third factor is imperfect growth condition. By adjusting parameter in MOCVD camber, we can increase tendency of lateral overgrowth. By solve these three problems, fully coalescent films could be possible to grow on our HNCP hollow beads coated sample with ultra-high coverage percentage. SEM images of partially detached GaN thin films and high-magnification cross section picture are shown in the Fig.23, Fig.24. From these images we can clearly observe the dense packed HNCP hollow beads structure. As a conclusion, self-assembly HNCP hollow silica particle pattern is successfully embedded with GaN thin films.

The PL spectra of sample grown on the bare sapphire substrate and HNCP hollow shell coated sapphire substrate are shown in Fig.25. PL spectra shows

that PL intensity is enhanced by 7 times by using hollow silica beads coated substrate. This enhancement is due to three factors, one is scattering effect of hollow silica beads, second is caused by higher crystal quality of GaN thin films, last one is by reason of scattering effect of rough surface. The main peak in the spectra corresponds to the near edge emission of GaN of c-plane. The shoulder peak in the hollow silica beads embedded films corresponds to the emission of semi-polar plane on GaN side wall without fully coalescent. Also peak of PL spectra is red shifted from 361.8nm to 363.5nm by using hollow silica beads coated substrate. This is due to the void provided by hollow silica shells reduce stress in GaN films.

The XRD spectra of sample grown on the bare sapphire substrate and HNCP hollow shell coated sapphire substrate are shown in Fig.26. In XRD measurement, FWHM value of (102) plane is reduced from 521.1 to 335.1 arcsec, but FWHM value of (002) plane is increase from 256.1 to 314.9 with using HNCP silica hollow beads coated substrate. FWHM values of (102) plane and (002) plane in GaN are related to the densities of edge dislocation and screw dislocation, respectively. Due to lateral overgrowth of GaN films, density of edge dislocation is significantly decreased by using HNCP silica hollow beads coated substrate. On the other hand, because growth condition is not fully optimized, and screw dislocations do not change their propagation direction in the lateral overgrowth mode, density of screw dislocation is increased.[13] We can conclude that crystal quality of GaN thin films is improved by using HNCP hollow silica beads coated substrate.

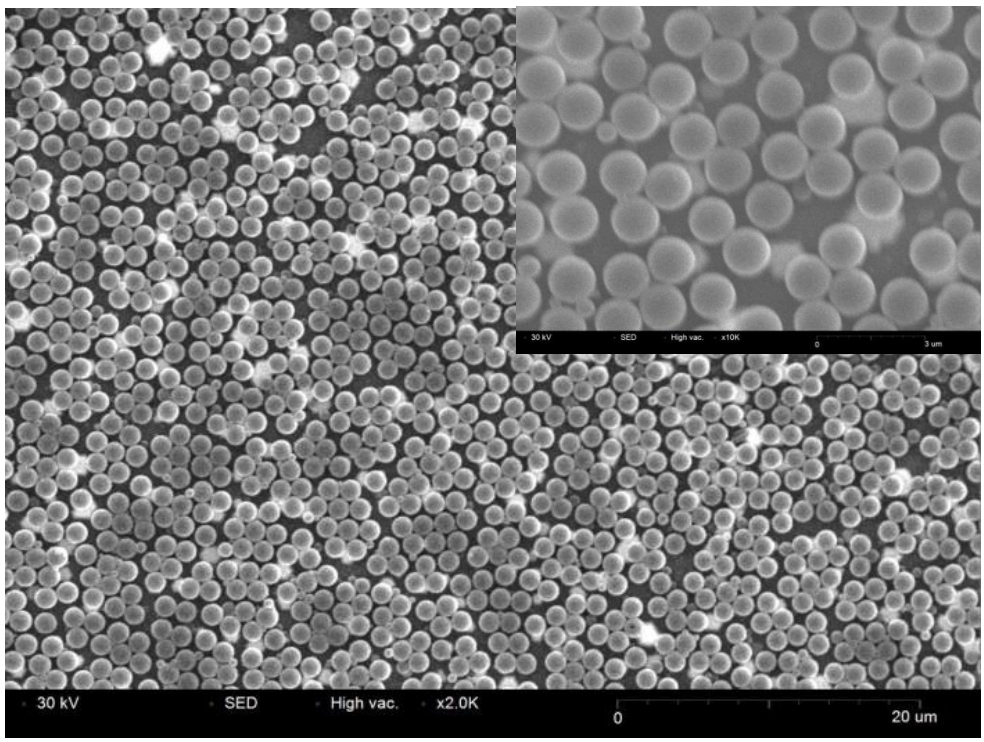

Figure 20 SEM images of nucleation process of GaN thin films (3 min growth).

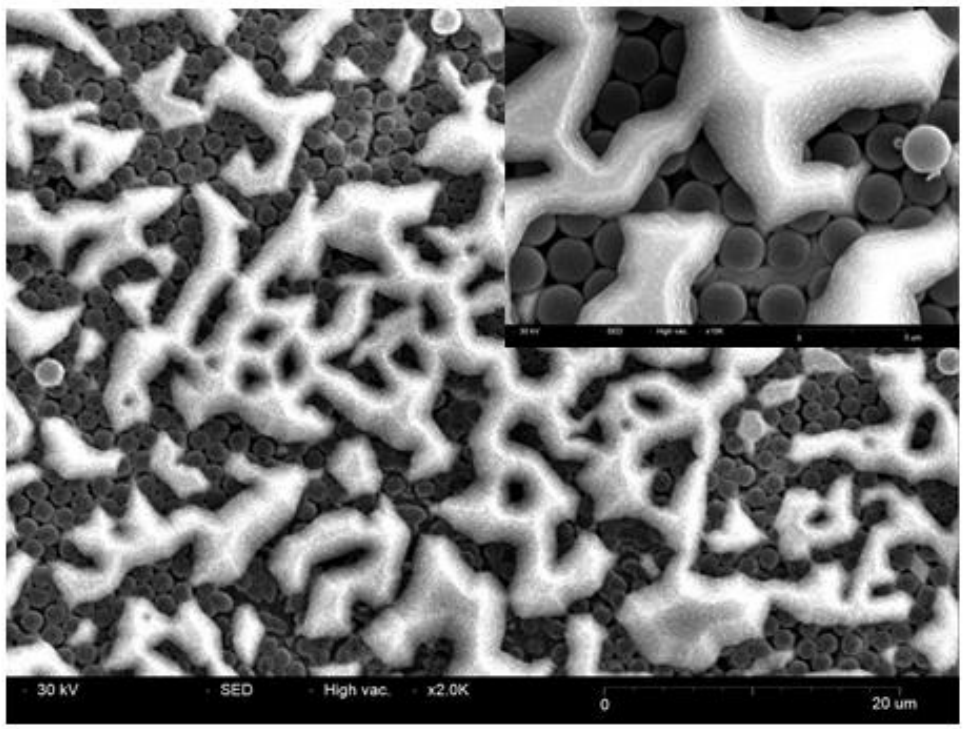

Figure 21SEM images of initial growth mode of GaN thin films (20min growth)

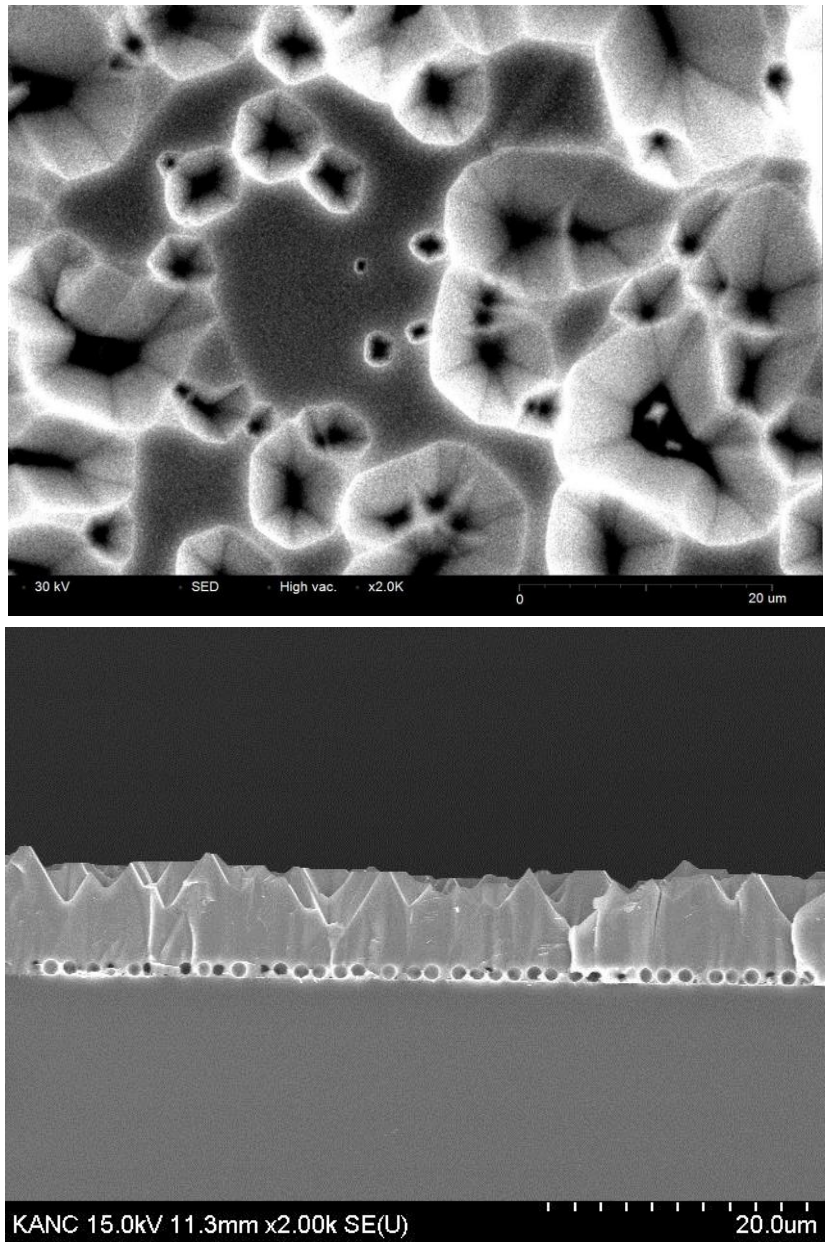

Figure 22 SEM images of plan and cross section view of GaN thin films (2.5h growth)

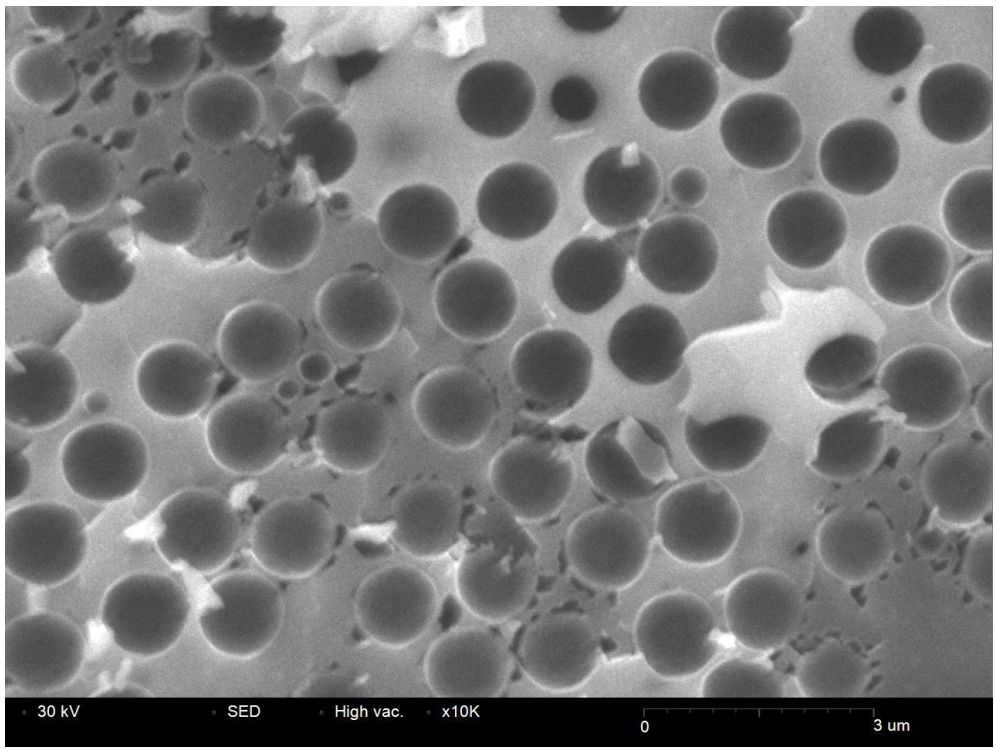

Figure 23 SEM images of partially detached GaN thin films

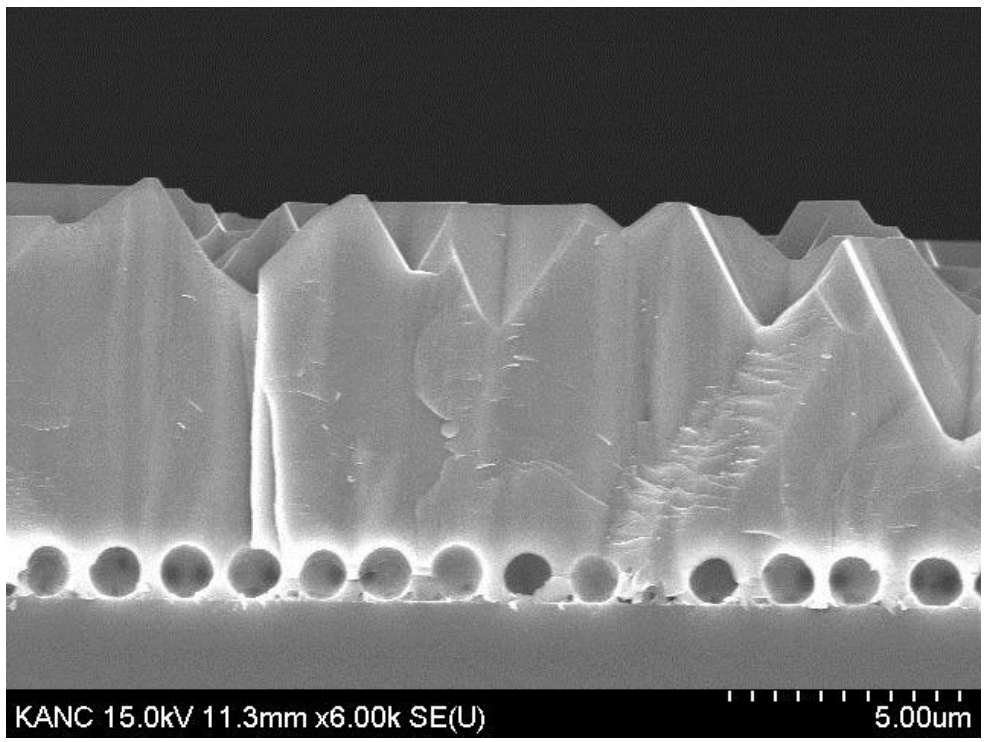

Figure 24 SEM image of high-magnification cross section of GaN film

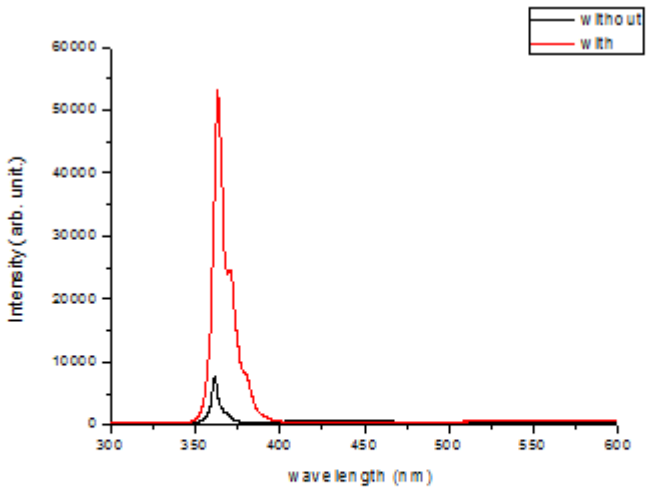

	Peak wavelength (nm)	Peak intensity
Without pattern	361.8	7604
With pattern	363.5	53100

Figure 25 PL spectra of sample grown on the bare sapphire substrate and HNCP hollow shell coated sapphire substrate

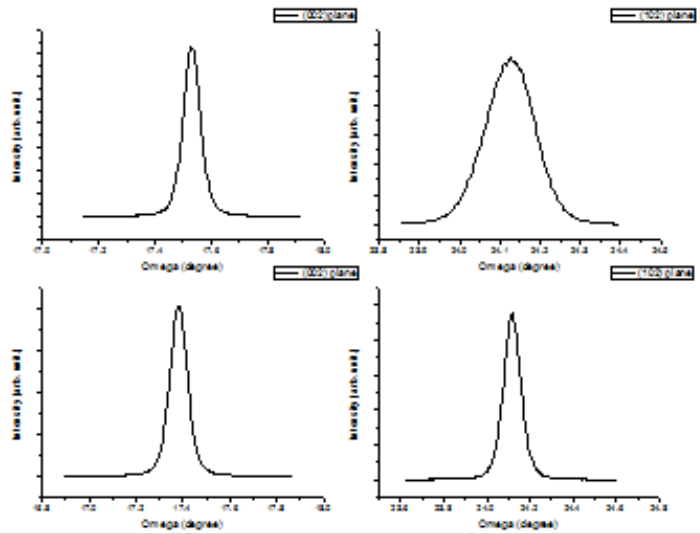

	FWHM of (002)	FWHM of (102)
Without pattern	256.1	521.1
With pattern	310.2	351.5

Figure 26 XRD spectra of sample grown on the bare sapphire substrate and HNCP hollow shell coated sapphire substrate

4.4 Conclusion

Self-assembly HNCP hollow silica particle pattern was successfully embedded with GaN thin films with ultra-high coverage percentage. Unfortunately, GaN thin films were not fully coalescent by current growth condition. Reasons are shown as follow. At first high coverage ratio of mask leaves less space for nucleation of GaN seed, then formation of films will become more difficult. Second factor is due to uniformity of films is not good enough. Existence of bilayer region or aggregate particles will also prevent both nucleation of GaN and lateral over growth. Third factor is imperfect growth condition. By adjusting parameter in MOCVD camber, we can increase the tendency of lateral overgrowth. By solve these three problems, fully coalescent films can be possible to grow on our HNCP hollow beads coated sample.

PL and XRD measurement shows that quality of GaN films was improved by embedding HNCP hollow silica shells. Light extraction was enhanced by scattering effect of HNCP hollow silica particle array. Stress of GaN films was also reduced by void provided by hollow particles.

Chapter 5.Conclusion

Various sized monodisperse shrinkable PS-silica core-shell beads was synthesized. By adjusting different experiment parameter, size of core-shell beads could be synthesized from 300nm to 3μm. effects on uniformity and size of amount of rpm, initiator, stabilizer, monomer, and co-monomer were investigated. Uniform polystyrene-MTC core was successfully synthesized and smooth silica shell was coated on the core.

By adjusting several experiment parameters in spin-coating process, sapphire substrate coated by monolayer core-shell particles with HCP structure was fabricated successfully. SEM images from region to region show that HCP monolayer was dominating in whole samples.

After thermal treatment, HCP core-shell particles array was transformed to HNCP hollow silica particles array. Depending on thermal treatment time, coverage percentage could be adjusted from 85% to 50%. Size of hollow shell decreased with longer heating time. PS-silica core-shell beads shrunk into a hollow silica shell with 55% size of as-synthesized particles at a minimum. Due to connection between neighboring particles, HNCP pattern was not perfect. These connection defects were inevitably formed during thermal treatment with low ramping time. However in the case of thermal treatment with high ramping time, like in MOCVD camber, connection between neighboring particles could be avoided.

Self-assembly HNCP hollow silica particle pattern was successfully

embedded with GaN thin films with ultra-high coverage percentage. Unfortunately, GaN thin films were not fully coalescent by current growth condition. GaN thin films could be expected to grow from HNCP patterned substrate by adjusting experiment condition or reducing coverage percentage of hollow silica shell.

PL and XRD measurement shows that quality of GaN films was improved by embedding HNCP hollow silica shells. Light extraction was enhanced by scattering effect of HNCP hollow silica particle array. Stress of GaN films was also reduced by void provided by hollow particles.

Reference

[1] C. A. Tran, R. F. Karlicek, M. G. Brown, I. Eliashevich, A. Gurary, M. Schurman, and R. Stall, Phys. Status Solidi A **176**, 91 (1999)

[2] T. Paskova, D.A. Hanser and K.R. Evans, Proceedings of the IEEE. **98.** 1324(2010)

[3] C.-L. Mo, W.-Q. Fang, Y. Pu, H.-C. Liu, and F.-Y. Jiang, J. Cryst. Growth **285**, 312 (2005)

[4] C. H. Wei, J. H. Edgar, C. Ignatiev, and J. Chaudhuri, Thin Solid Films **360**, 34 (2000)

[5] D. S. Li, H. Chen, H. B. Yu, H. Q. Jia, Q. Huang, and J. M. Zhou, J. Cryst. Growth **267**, 395 (2004)

[6] S. Nakamura, M. Senoh, S. Nagahama, N. Iwasa, T. Yamada, T. Matsushita, H. Kiyoku, and Y. Sugimoto, Appl. Phys. Lett. **68**, 2105 (1996)

[7] L. Wang, S. Tripathy, B. Wang, J. Teng, S. Chow, and S. Chua, Appl.Phys. Lett. **89**, 011901 (2006)

[8] S. J. Pearton, J. C. Zolper, R. J. Shul and F. Ren , J. Appl. Phys. **86,** 1, (1999)

[9] N. G. Weimann, L. F. Eastman, D. Doppalapudi, H. M. Ng, and T. D. Moustakas, J. Appl. Phys. **83**, 3656 (1998)

[10] T. Sugahara, H. Sato, M. S. Hao, Y. Naoi, S. Kurai, S. Tottori, K. Yamashita,K. Nishino, L. T. Romano, and S. Sakai, Jpn., Part2 **37**, L398 (1998)

[11] S. Tomiya, M. Takeya, S. Goto, and M. Ikeda, Mater. Res. Soc. Symp.Proc. **831**, 3 (2005)

[12] S.S. Schad, M. Scherer, M. Seyboth and V. Schwegler. Phys. Stat. Sol. (a), **188**, 127(2001)

[13] J.K. Kim, H.J. Woo, K.S. Joo, S.W Tae, J.S Park, D.Y Moon, S.H Park, J.H Jang, Y.G Cho, J.C Park, H.K Yuh, G.D Lee, I.S Choi, Y. Nanishi, H.N. Han, K.Char and E.J. Yoon. SCIENTIFIC REPORTS **3**, 3201(2013)

[14] T.S. Zheleva, O.K. Nam, M.D. Bremser and R.F. Davis. Appl. Phys. Let, **71**, 2472(1997)

[15] O.K. Nam, M.D. Bremser, T.S. Zheleva and R.F. Davis. Appl. Phys. Let **,71**, 2638(1997)

[16] T.S Oh, S.H. Kim, T.K. Kim, Y.S. Lee, H. Jeong, G.M. Yang and E.K. Suh, et al. Jpn. J. Appl. Phys., **7**, 5333(2008)

[17] J.J. Chen, Y.K. Su, C.L. Lin, S.M. Chen, W.L. Li and C.C. Kao, IEEE photonics technology letters. **20**, 1993(2008)

[18] Y.J. Lee, H.C.Kuo, T.C. Lu, S.C. Wang, K.W. Na, K.M. Lau and Z.P. Yang,. Light Technology. **26**, 1445(2008)

[19] C.C Pan, C.H. Hsieh, C.W. Lin and J.J. Chyi Appl. Phys. Let, **102**, 084503(2007)

[20] S. J. An, Y. J. Hong, G. Yi, Y.J. Kim, and D. K. Lee, Adv. Mater., **18**, 2833–2836 (2006)

[21] K. Ueda, Y. Tsuchida, N. Hagura, F. Iskandar, K. Okuyama, and Y. Endo, Appl. Phys. Let, **92**, 101101 (2008)

[22] Q. Li, J.J. Figiel, and G. T. Wang, Appl. Phys. Let, **94**, 231105 (2009)

[23] S. H. Park, J. Park, D.-J. You, K. Joo, D. Moon, J. Jang, D.-U. Kim, H. Chang, S.

Moon, Y.-K. Song, G.-D. Lee,H. Jeon, J. Xu, Y. Nanishi, and E. Yoon, Appl. Phys. Let, **100**, 191116 (2012)

[24] H. Zou, S. Wu and J. Shen, Chem. Soc. ReV. **27**, 1 (1998)

[25] M. Yasuda, H. Seki, H.Yokoyama, H. Ogino, K. Ishimi and H. Ishikawa, Macromolecules, **34**, 3261(2001)

[26] M. Chen, L. Wu, S. Zhou, and B. You, Adv. Mater., **18**, 801–806 (2006)

[27] J. Lee, C.K.Hong, S.Choe, and S.E. Shim, J. Col. Inter. Sci., **310**, 112 (2007)

[28] A. Schmid, S. Fujii, and S.P. Armes, Langmuir, **22**, 4923(2006)

[29] F. Caruso, R.A. Caruso, and H.Mohwald, Science **282**, 1111(1998)

[30] Y. Lu, J. McLellan, and Y. Xia, Langmuir, **20**, 3464, (2004)

[31] M. Chen, S. Zhou, L. Wu, S. Xie and Y. Chen. Macromol, Chem. Phys. 206, 1896 (2005)

[32] J. Xu, P. Li and C. Wu, J. Polym. Sci. Part A Polym. Chem. **37**, 2069 (1999)

[33] D. Horak, Acta Polymer. **47**, 20 (1996)

[34] F.Zhang, Y. Bai, Y. Ma and W. Yang, J. Col. Inter. Sci., **334**, 13(2009)

[35] J. Weissman, H.Sunkara, A. S. Tse, S. A Asher, Science, **274**, 959. (1996)

[36] Y.Xia, B. Gates, Y. Yin, and Y. Lu, Adv. Mater., **12**, 693. (2000)

[37] J. C. Hulteen and R. P. Vanduyne, J. Vac. Sci. Technol. A **13**, 1553 (1995)

[38] P. Jiang, Appl. Phys. Lett., **89**, 011908.(2006)

[39] J. Aizenberg, P. V. Braun, and P. Wiltzius, Phys. Rev. Lett. **84**, 2997 (2000)

[40] P.I. Stavroulakis, N. Christou, and D. Bagnall, Materials Science and Engineering B **165,** 186–189 (2009)

[41] S.M. Weekes, F.Y. Ogrin, W.A. Murray, P.S. Keatley, Langmuir **23** 1057–1060 (2007)

[42] D. G. Choi, H. K. Yu, S. G. Jang, and S. M. Yang, J. Am. Chem. Soc. **126**, 7019 (2004)

[43] A. van Blaaderen, R. Ruel, and P. Wiltzius, Nature London **385**, 321 (1997)

[44] D. G. Grier, Nature London **424**, 810 (2003)

[45] X. Yan, J. M. Yao, G. Lu, X. Li, J. H. Zhang, K. Han, and B. Yang, J. Am. Chem. Soc. **127**, 7688 (2005)

[46] W. D. Ristenpart, I. A. Aksay, and D. A. Saville, Phys. Rev. Lett. **90**, 128303 (2003)

[47] T. Ogi, L.B. Modesto-Lopez, F. Iskandar, and K. Okuyama, Colloids and Surface A. **297**, 71 (2007)

[48] N. D. Dendov, O. D. Velev, P. A. Kralchevsky, and I.B. Ivanov, Langmuir, **8**, 3183 (1992)

[49] P. Colson et al. Langmuir, **27**, 12800–12806 (2011)